

Optical properties of cubic SiC grown on Si substrate by chemical vapor deposition

Zhe Chuan Feng *

Graduate Institute of Electro-Optical Engineering and Department of Electrical Engineering, National Taiwan University, Taipei 106-17, Taiwan, ROC

Available online 18 November 2005

Abstract

A series of 3C-SiC films with varied film thickness up to 17 μm have been grown on Si(100) by chemical vapor deposition, and studied by photoluminescence, Raman scattering, Fourier transform infrared transmission and reflectance measurements. Typical key behaviors on these optical spectra are investigated. Thinner ($<3 \mu\text{m}$) films have their optical spectral features, mainly associated with defects. High quality of single crystalline cubic SiC materials can be obtained from thicker ($>10 \mu\text{m}$) films, evidenced by optical spectra. There exists a tensile stress in the 3C-SiC film grown on Si, affecting greatly the optical features. Its measurements have led to a formulas on two deformation potentials, a and b .

© 2005 Elsevier B.V. All rights reserved.

Keywords: 3C-SiC; Si; Chemical vapor deposition; Photoluminescence; Raman scattering; Fourier transform infrared spectroscopy

1. Introduction

Silicon carbide (SiC) and its polytypes are promising semiconductors for high temperature, high frequency and high power electronic and optoelectronic applications, which have raised a great deal of research and development (R&D) interests [1–3]. During the last few years significant progress has been achieved in the development of 4H and 6H wafers and related devices. However, the cost of 4H and 6H-SiC wafers remains high. Also, some technique bottlenecks exist, such as high density of micro-pipes and deep traps due to strain accumulation, doping striations and domain misorientation, which greatly reduce the effective device mobility and limit the device performance [4].

Among all SiC polytypes, cubic silicon carbide (3C-SiC) exhibits the highest electron mobility [5], and is the only material that can be grown on low-cost Si substrate [6] and with a potential to merge into the well-developed Si-base integration technology. It has many advantages for

MOS device applications permitting “inversion” at lower electric field strength and free of electron traps generated by the “near interface-trap effect” [4]. Nano-structural 3C-SiC has recently approved to exhibit the enhanced blue emissions due to the quantum confinement effect [7]. By way of chemical vapor deposition (CVD), the successful growth of 3C-SiC films on Si wafers has been achieved in 1983 [8] by overcoming the difficulties from the large lattice difference of about 20% and an 8% mismatch in the thermal expansion coefficients between 3C-SiC and Si [9]. The author has recently published a book chapter [10] to review, and introduced important research and development (R&D) on 3C-SiC materials growth and analyses since 1983. However, beyond those references till 2003, cited in [10], many attractive and interesting results on 3C-SiC R&D are reported in 2004–2005 [4,5,7,11–19] and more are coming.

In this paper, we present an investigation on the optical properties of CVD-grown 3C-SiC/Si materials by way of photoluminescence (PL), Raman scattering, and Fourier transform infrared (FTIR) spectroscopy. Typical data are presented to express the main features of optical spectra from CVD 3C-SiC/Si.

* Tel.: +886 2 3366 3543; fax: +886 2 2367 7467.

E-mail address: zcfeng@cc.ee.nut.edu.tw.

2. Experimental

The experimental samples involved in this paper were prepared by chemical vapor deposition (CVD). This CVD procedure produces an initial SiC layer from a carbonization, which was done by way of an initial temperature ramp on the Si substrate in the presence of a hydrocarbon [9]. This thin (\sim several hundreds of angstrom) SiC mixed alloy layer served as a buffer for a subsequent CVD growth of SiC.

For the characterization of studied materials, low temperature (LT) photoluminescence (PL) measurements were performed at ~ 2 K with the sample immersed in pumped liquid He, a He–Cd laser or a filtered Hg lamp for UV excitation, a SPEX-1400 spectrometer for signal light dispersion, a photomultiplier for detection, a lock-in amplifier and related electronics and computer for signal magnification and processing [20]. Raman scattering was measured in the near backscattering geometry, with excitations from an Ar ion laser, and using a triple spectrometer – optical multichannel analyzer system. FTIR spectra were measured by a Perkin–Elmer 2000 FTIR spectrometer.

3. Results

3.1. Low temperature photoluminescence

Fig. 1 shows 2 K PL spectra for three CVD 3C-SiC/Si(100) samples with SiC film thickness, d , of 3.2, 4 and

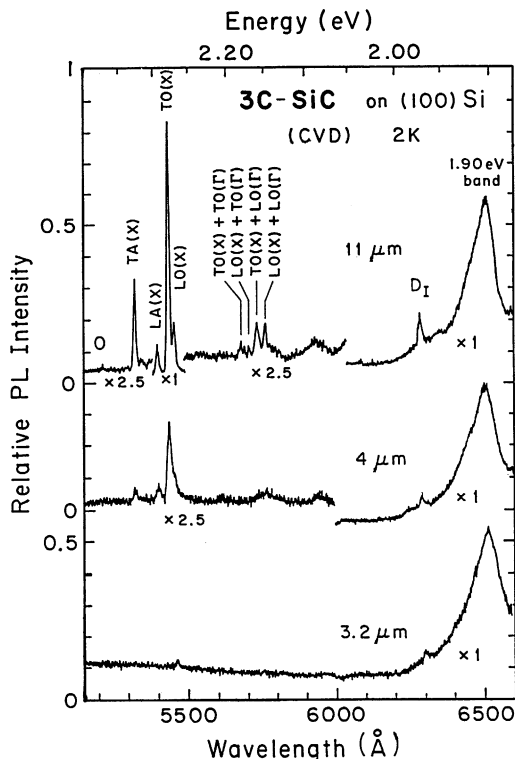


Fig. 1. 2 K photoluminescence spectra of three CVD 3C-SiC/Si(100) with $d = 3.2, 4$ and $11 \mu\text{m}$.

$11 \mu\text{m}$, respectively. The thinnest film showed a dominant 1.90 eV PL band, i.e., the so-called G band, plus a weak D_I band at 1.972 eV and weak emissions near 2.15 eV, all of which are defect-related features in 3C-SiC [20]. As the film becomes thicker, exciton lines appear in the wavelength range of 5200–5500 Å. As the film is thicker than $10 \mu\text{m}$, the non-zero phonon line, labelled “O” appears, the nature of which is due to the exciton bound to neutral nitrogen donors. Its first order phonon replicas, labelled as TA(X), LA(X), TO(X) and LO(X), appear sharply. Their second-order combinations can also be observed. The observation of exciton lines is characteristic of the good quality of experimental samples.

3.2. Raman scattering

Fig. 2 shows Raman spectra for three 3C-SiC/Si(100) samples with LT-PL displayed in Fig. 1. We see, as $d(\text{SiC})$ increases from 4 to $11 \mu\text{m}$, the intensities of 3C-SiC longitudinal optical (LO) and transverse optical (TO) phonon modes increase, with respect to that of the Si substrate. For the poor quality one with $d(\text{SiC}) = 3.2 \mu\text{m}$, the allowed LO mode is weaker than the forbidden TO mode. Also, some extra features exist, corresponding to other polytypes of SiC or defects. After removal of Si substrate, the LO and TO lines will shift their position a little. These Raman line shifts can be used to determine the stress and strain inside the 3C-SiC films [21]. The relationship between the Raman feature and film quality can be established [22].

3.3. Fourier transform infrared spectroscopy

Fourier transform infrared (FTIR) spectroscopy was used to study the initial growth of 3C-SiC films. Fig. 3(A) shows FTIR transmission spectra for four CVD 3C-SiC/Si(100) with different growth time or different film thickness. For a very thin film with the growth time, τ , of only 2 min, a transmission band near 800 cm^{-1} in Fig. 3(A, curve a) indicates the initial stage

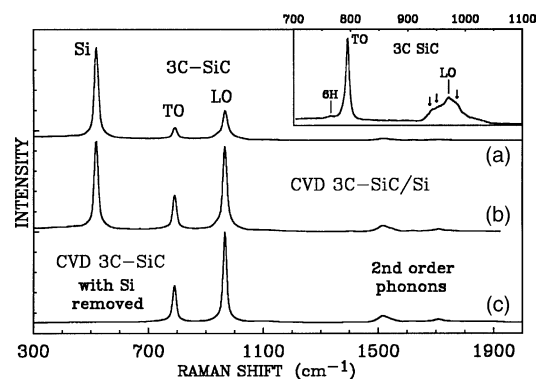


Fig. 2. Raman spectra of three CVD 3C-SiC grown on (100) Si with the film thickness of $3.2 \mu\text{m}$ (right-up corner), (a) $4 \mu\text{m}$, (b) $11 \mu\text{m}$, and (c) $11 \mu\text{m}$, with the Si substrate removed.

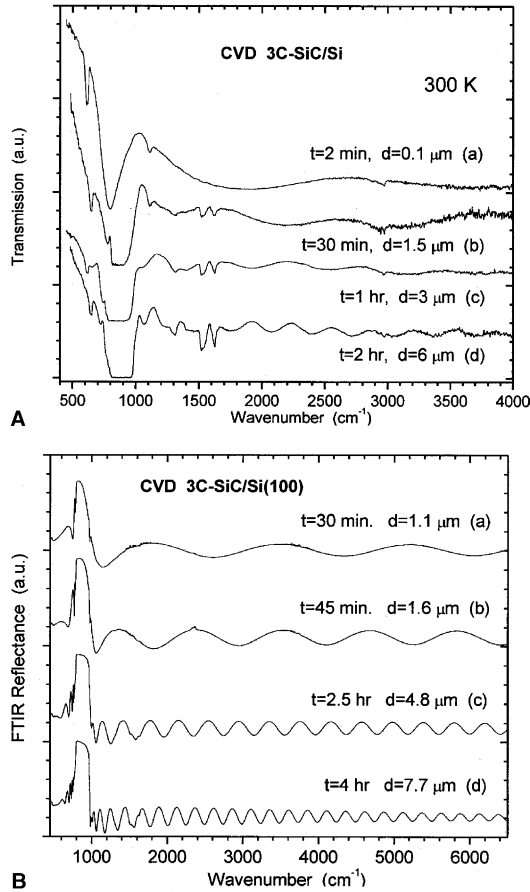


Fig. 3. Fourier transform infrared (FTIR) spectra of: (A) transmission from four CVD 3C-SiC/Si(100) with film thickness of 0.1, 1.5, 3 and 6 μm and (B) reflectance from four CVD 3C-SiC/Si(100) with film thickness of 1.1, 1.6, 4.8 and 7.7 μm , respectively.

of the formation of the SiC-like crystal but not true 3C-SiC yet. As τ increases to 30 min, a deep and flat band between 770 and 920 cm^{-1} appears in Fig. 3(A, curve b), with both edges corresponding to the TO and LO phonon frequencies. This characterizes the complete formation of 3C-SiC. As τ increases to 1 and 2 h, i.e., with the film thickness increased to 3 and 6 μm , respectively, this reststrahlen band becomes further broad and flat, indicating the improvement of the cubic crystalline perfection of the 3C-SiC layers grown on Si substrate.

FTIR reflectance spectroscopy can also be employed for the materials evaluation of CVD-grown 3C-SiC films on Si. Fig. 3B shows FTIR reflectance spectra from another set of four CVD 3C-SiC/Si(100) with different growth time or film thickness of 1.1, 1.6, 4.8 and 7.7 μm , respectively. Theoretical simulation can be applied to the 3C-SiC/Si system to give more information on the material properties [23].

4. Discussion

We are giving a further discussion from luminescence features on the experimentally observed shifts of N-BE lines and the effects of a tensile biaxial stress on bound exci-

ton transitions. The lattice constant of 3C-SiC at RT is 4.359 \AA and is smaller than that of Si (5.430 \AA at RT). The thermal expansion coefficient of 3C-SiC is slightly larger than that of Si [10]. Consequently, as an epitaxial 3C-SiC film is grown on a Si substrate by CVD, we have a tensile biaxial stress inside the SiC film. Our Raman scattering studies [10,20] have shown that this tensile biaxial stress shifts the optical phonons of 3C-SiC to lower energies. According to the theoretical analyses in [20], it also splits the $\mathbf{k} = 0$ (Γ point) degenerate valence band, puts the heavy-hole band on top and narrows the energy band gap. The band gap change, ΔE_g , due to a tensile biaxial stress, X , can be calculated by a formula [10,20],

$$\begin{aligned} \Delta E_g &= \delta E_h - (1/2)\delta E_s \\ &= X[2a(S_{11} + 2S_{12}) + b(S_{11} - S_{12})], \end{aligned} \quad (1)$$

where δE_s is the energy splitting between the heavy-hole and light-hole bands, a is the hydrostatic-pressure deformation potential and b is a uniaxial deformation potential, S_{11} and S_{12} are the compliances of 3C-SiC, respectively. For the case of 3C-SiC/Si with a tensile stress, $X > 0$, the values of a and b are negative, we have $\Delta E_g < 0$ in Eq. (1). This conclusion can be directly confirmed from our PL measurements in Fig. 4 for a comparison of 2 K PL spectra for nitrogen-bound-exciton (N-BE) peaks between a 3C-SiC/Si and a 3C-SiC free film with similar thicknesses. The N-BE and phonon replicas from 3C-SiC on Si shift to

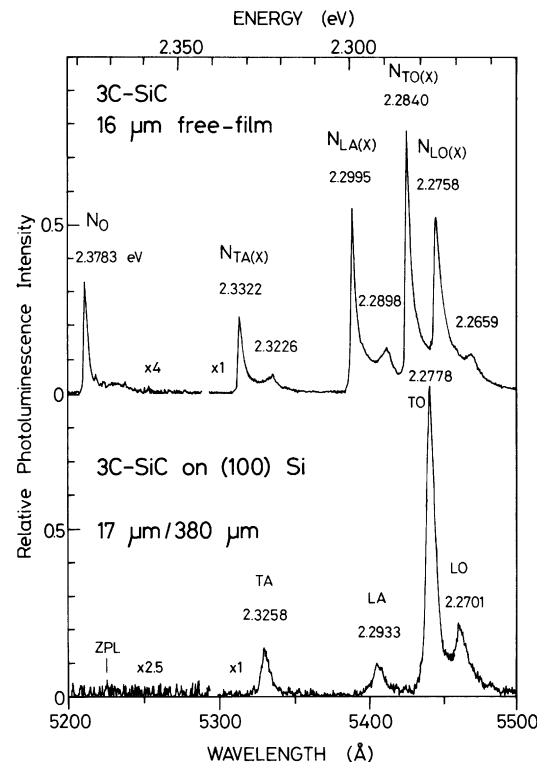


Fig. 4. Comparative 2 K PL spectra for nitrogen-bound-exciton (N-BE) peaks from two 3C-SiC films of (top) a 16- μm thick free film and (bottom) a 17 μm film on Si(100).

longer wavelength, i.e., lower energies in comparison with 3C-SiC free films in the figure.

Because the 3C-SiC deformation potentials of a and b are not available, we cannot use Eq. (1) to calculate the stress inside the 3C-SiC film on Si. However, we have an estimate of the values of stress X from our previous Raman measurements [21] and here we observe line shifts presumably related to the band gap shift ΔE_g from the PL measurement. This enables us to make a rough estimate of the range of the deformation potentials in 3C-SiC. Also, the compliances values of 3C-SiC from the literature are in scatter [24–27]. In earlier studies [20,21], we used the values of $S_{11} = 2.22 \times 10^{-13} \text{ cm}^2/\text{dyn}$ and $S_{12} = -0.56 \times 10^{-13} \text{ cm}^2/\text{dyn}$ for 3C-SiC from [25] and obtained an estimate of

$$2.2a + 2.8b \sim -10 \text{ eV}. \quad (2)$$

Recently, Rohmfeld et al. [28], considering the case of non-zero components of uniaxial stress–strain in the normal direction of the film, have recently performed an accurate measurement of the biaxial stress–strain by using a pressure sensor and tuning the biaxial strain via applying a differential nitrogen pressure, on two 3C-SiC membranes (1.5 and 1.8 μm thick, respectively), and obtained Raman stress coefficients of 3C-SiC. In their work, the values of calculated Raman hydrostatic stress coefficients [27] and the calculated elastic compliance constants from Tolpygo [25] were used, i.e.,

$$S_{11} = 3.67 \times 10^{-3}/\text{GPa} \quad \text{and} \quad (3)$$

$$S_{12} = -1.05 \times 10^{-3}/\text{GPa}.$$

With these values, and $X = 0.61 \text{ GPa}$ from Raman analysis and $\Delta E_g = -6.2 \text{ meV}$ from Fig. 4 for this sample, we have from Eq. (1),

$$3.1a + 4.7b \sim -10 \text{ eV}, \quad (4)$$

or approximately,

$$3a + 5b \sim -10 \text{ eV}, \quad \text{i.e., } 0.6a + b \sim -2 \text{ eV}, \quad (5)$$

where the deformation potentials a and b are in units of eV. Eq. (4) or Eq. (5) should replace Eq. (12) in [7] or Eq. (2) given above.

In additions to the variation of the N-BE line positions, Fig. 4 also showed the variations of their relative line intensities due to the tensile stress. For examples, the zero-phonon line is almost completely depressed by the stress, and TA–LA–TO phonon replicas lines are attenuated much more than the TA line. We will explore to penetrate further on these phenomena in the near future.

5. Conclusion

In conclusion, we have performed photoluminescence (PL), Raman scattering (RS), Fourier transform infrared (FTIR) transmission and reflectance measurements of a series of CVD-grown 3C-SiC/Si samples with varied film thickness up to 17 μm . Typical key or main features on

these optical spectra are obtained. It has shown that the thinner (less than 3 μm) 3C-SiC grown on Si have their PL, RS and FTIR optical spectral features, mainly associated with defects. After a certain thickness ($>10 \mu\text{m}$) of CVD film growth, good and high quality of single crystalline cubic SiC films on Si were obtained, evidenced by PL, RS and FTIR spectra.

From comparative measurements for 3C-SiC grown on Si and with Si substrate removed, the stress and strain effects on 3C-SiC/Si are exposed. Tensile stress in the 3C-SiC films grown on Si is identified and measured. A relation formulas on two deformation potentials, a and b , for 3C-SiC is deduced from the PL and Raman data. Further interesting variations on the intensities from bound exciton lines of 3C-SiC due to layer tensile stress are described, to be studied further.

Acknowledgments

The author acknowledges the supports and help in this work from Profs. (Drs.) W.J. Choyke, J.A. Powell, S. Perkowitz, D.N. Talwar, C.C. Tin, J. Lin, S.J. Chua, and C.C. Yang. The work at National Taiwan University was supported by funds from National Science Council of Republic of China, NSC 93-2218-E-002-011 and 93-2215-E-002-035.

References

- [1] W.J. Choyke, H. Matsunami, G. Pensl (Eds.), *Silicon Carbide: Recent Major Advances*, Springer, Berlin, 2004.
- [2] Z.C. Feng, J.H. Zhao (Eds.), *Optoelectronic Properties of Semiconductors and Superlattices*, M.O. Manasreh (Chief Ed.), Taylor & Francis Books Inc., New York, 2003. *Silicon Carbide: Materials, Processings and Devices*, vol. 20.
- [3] Z.C. Feng (Ed.), *SiC Power Materials – Devices and Applications*, Springer, Berlin, 2004.
- [4] E. Polychroniadis, M. Syväjärvi, R. Yakimova, J. Stoemenos, *J. Cryst. Growth* 263 (2004) 68.
- [5] M. Eickhoff, H. Möller, J. Zappe, G. Kroetz, *J. Appl. Phys.* 95 (2004) 7908.
- [6] H. Nagasawa, K. Yagi, T. Kawahara, *J. Cryst. Growth* 237–239 (2002) 1244.
- [7] X.L. Wu, J.Y. Fan, T. Qiu, X. Yang, G.G. Siu, P.K. Chu, *Phys. Rev. Lett.* 94 (2005) 026102.
- [8] S. Nishino, J.A. Powell, H.A. Will, *Appl. Phys. Lett.* 42 (1983) 460.
- [9] J.A. Powell, P. Pirouz, W.J. Choyke, Growth and characterization of silicon carbide polytypes for electronic applications, in: Z.C. Feng (Ed.), *Semiconductor Interfaces, Microstructures and Devices: Properties and Applications*, Institute of Physics Publishing, Bristol, 1993, p. 257.
- [10] Z.C. Feng, Characterization of Cubic SiC Grown on Si by Chemical Vapor Deposition, in [3], 2004, pp. 209–276.
- [11] H. Nagasawa, K. Yagi, T. Kawahara, N. Hatta, G. Pensl, W.J. Choyke, T. Yamada, K.M. Itoh, A. Schöner, Low-defect 3C-SiC Grown on Undulant-Si (001) Substrates, in [1], pp. 207–228.
- [12] Y. Dong, P. Molian, *Appl. Phys. Lett.* 84 (2004) 10.
- [13] P. Djemia, Y. Roussigné, G. Dirras, K.M. Jackson, *J. Appl. Phys.* 95 (2004) 2324.
- [14] T. Nishiguchi, M. Nakamura, K. Nishio, T. Isshiki, S. Nishino, *Appl. Phys. Lett.* 84 (2004) 3082.

- [15] T.J. Fawcett, J.T. Wolan, R.L. Myers, J. Walker, S.E. Sadow, *Appl. Phys. Lett.* 85 (2004) 416.
- [16] G. Wang, B. Wang, A. Huang, M. Zhu, M. Yu, H. Yan, *J. Cryst. Growth* 267 (2004) 173.
- [17] R. Püsche, M. Hundhausen, L. Ley, K. Semmelroth, F. Schmid, G. Pensl, H. Nagasawa, *J. Appl. Phys.* 96 (2004) 5569.
- [18] I. Szlufarska, R.K. Kalia, A. Nakano, P. Vashishta, *Appl. Phys. Lett.* 86 (2005) 021915.
- [19] J.Y. Fan, X.L. Wu, F. Kong, T. Qiu, G.S. Huang, *Appl. Phys. Lett.* 86 (2005) 171903.
- [20] W.J. Choyke, Z.C. Feng, J.A. Powell, *J. Appl. Phys.* 64 (1988) 3163.
- [21] Z.C. Feng, W.J. Choyke, J.A. Powell, *J. Appl. Phys.* 64 (1988) 6827.
- [22] Z.C. Feng, C.C. Tin, R. Hu, J. Williams, *Thin Solid Films* 266 (1995) 1.
- [23] Z.C. Feng, W.Y. Chang, S.J. Chua, J. Lin, C.C. Tin, in: N. Miura, T. Ando (Eds.), *Proceedings of the 25th International Conference on the Physics of Semiconductors*, Springer Proceedings in Physics, vol. 87, Springer-Verlag, Berlin, 2001, p. 1559.
- [24] K.B. Tolpygo, *Sov. Phys. – Sol. State* 2 (1960) 2367.
- [25] G.A. Slack, *J. Appl. Phys.* 35 (1964) 3460.
- [26] M. Miura, H. Murata, Y. Shiro, K. Lishi, *J. Phys. Chem. Solids* 42 (1981) 931.
- [27] D.H. Lee, J.D. Joannopoulos, *Phys. Rev. Lett.* 48 (1982) 1846.
- [28] S. Rohmfeld, M. Hundhausen, L. Ley, C.A. Zorman, M. Mehregany, *J. Appl. Phys.* 91 (2002) 1113.